

# Geotechnical Investigation, Modelling and Visualization of Shallow Subsurface Soil at Khobash District, Najran, Saudi Arabia

Adnan Aqeel<sup>\*1,2</sup>, Stanley Nwokebuihe<sup>3</sup>, Saleh Qaysi<sup>4</sup>, Ahmed Abd El-Al<sup>5,6</sup>, Adel Elkrry<sup>7</sup>

<sup>1</sup>Dept. of Geology, College of Science, Taibah University, P.O. Box 30002, Madinah, Zip Code: 41477

<sup>2</sup>Dept. of Earth and Environmental Sciences, Faculty of Science, Sana'a University, Yemen

<sup>3</sup>Faith Technologies Inc., Huntsville, AL, USA

<sup>4</sup>Geology and Geophysics Dept., King Saud University, Riyadh, Saudi Arabia

<sup>5</sup>Geology Dept. Al Azhar University (Assiut Branch), Assiut, Egypt

<sup>6</sup>Dept. of Civil Engineering, Najran University, Najran, Saudi Arabia

<sup>7</sup>Dept. of Geology and Applied Geophysics, University of Al-Jabel Al-Gharibi, Libya

Received 23<sup>rd</sup> March 2022; Accepted 26<sup>th</sup> September 2022

## Abstract

2D and 3D Geotechnical models of the top 10-meter depth of the study area were created to reflect the investigated geotechnical spatial variation behavior of subsurface soil. The geotechnical investigation included advancing boreholes down to 10 m at 50 stations reflecting the resistance of soil (N-value) and collecting 250 soil samples at different depths to identify soil geotechnical properties. For foundation construction purposes, 15 random test pits were also excavated down to 3 m depth to mainly measure soil compaction parameters.

Soil particles of sand (61 – 99%) silt (0 – 26%), and gravel (0 – 23%), with no clay particles, were identified in the area; thus, the soils were classified into SP, SP-SM, and SM. These soils also have shown a wide range of water content (2.90 – 20.10%), N-value (13 – 85), relative density (medium to very dense), maximum dry density (2.0- 2.2 g/cm<sup>3</sup>), and an internal friction angle of 25° to 28°.

The produced geotechnical models have made correlation and linking spatial variations of geotechnical properties with each other, and even within each property, an easy and significant task. Therefore, producing such geotechnical models was a powerful and useful technique to interpret and predict the geotechnical behavior of subsurface soil.

© 2023 Jordan Journal of Earth and Environmental Sciences. All rights reserved

**Keywords:** Geotechnical Investigation, Subsurface Soil, Spatial Variation, 2D geotechnical Models, 3D geotechnical Models, Najran

## 1. Introduction

Earthen materials have commonly wide variations in their geological and geotechnical properties which can lead to severe geotechnical problems and hazards and even cause catastrophic events. Therefore, accurate assessment of the uncertainty of engineering behavior is an important phase of all civil engineering projects particularly for those projects which involve significant interactions with subsurface earthen materials (Parsons et al., 2002). In recent years, many human-made geohazards, such as ground subsidence, engineering slope instability and foundation settlements, have been witnessed with more regularity in growing urban areas due to the lack of adequate and accurate subsurface geological and geotechnical studies, resulting in threats to human lives and properties (Tang and Xu, 2009; Dong et al., 2015; Aqeel et al., 2019; Abd El Al et al., 2019, 2020).

In general, the in-situ geotechnical behavior of subsurface soils is complex and heavily dependent on the nexus of factors related to the complicated nature and exacerbated by human practices (Breysse et al., 2005; Massoud, 2016). Therefore, engineering geologists and civil engineers have been facing a challenge on how to clarify and accurately depict and

visualize the underground surface conditions considering, at the same time, the horizontal and vertical distributions, and variations of geotechnical parameters.

Although producing traditional geological and geotechnical maps (2D models) has been intensely used to visualize ground conditions in fields of geoengineering, geology, and civil engineering (Kanu et al., 2013; Ayodele and Ajigo, 2020; Khallouf et al., 2020; Tobore et al., 2023), one of the biggest limitations is that these 2D models are restrictive in their ability to depict the subsurface across a range of depths and to chart the variations in geotechnical properties underground (Ding et al., 2015). In contrast, creating three-dimensional (3D) models with a thickness corresponding to different depths of interest can be integrated with various geotechnical, geological, hydrogeological, and geometrical parameters. As a result, representation, visualization, analysis, and interpretation of the underground conditions can be accurately conducted (Ford et al., 2008; Roysse et al., 2009; Thierry et al., 2009; Dong et al., 2015).

Furthermore, the 3D geotechnical model is distinguished by including both a boundary model, which delineates the boundary between the different defined subsurface

\* Corresponding author e-mail: ben\_aqeel\_2005@yahoo.com

geotechnical units, and a property model, which depicts the spatial distribution and variation of the geotechnical properties within those defined units (Hack et al., 2006).

Briefly, creating a 3D Model of the distribution of the geotechnical properties of the subsurface is increasingly becoming crucial in the decision-making process for commercial development and urban planning and management. It is not only a cost-effective method for characterizing the earth's subsurface in geoenvironmental and civil engineering design practices but also it is an effective way to save effort and time in the analysis of data. Moreover, producing such subsurface geotechnical modeling is crucial for environmental risk assessment especially in rapidly growing cities (Mends and Lorandi, 2008; Kolat et al., 2006, 2012; Donghee et al., 2012; Abd El Aal and Rouaiguia, 2020).

All aforementioned studies pointed out the main objective of creating these 3D subsurface geotechnical models, which is usually to analyze and visualize the investigated geotechnical parameters of the area of interest concerning its vertical extension and thus to effectively assess its geotechnical performance.

Accordingly, most potential critical zones can be accurately depicted and identified. Hence, such information could result in the optimization of the proper design process of a construction as well as it could actively assist in reducing the construction risks.

In this research, geotechnical investigation and analysis, and producing of geotechnical spatial variations models (2D and 3D models) of the shallow subsurface soil of Khobash district, Najran Province, were conducted. Briefly, the main objectives of this research are to address the geotechnical properties of the study area concerning its vertical extension (depths), to correlate and link horizontal and vertical spatial variations of the investigated geotechnical properties with each other and even within each property, and thus to predict its geotechnical behavior as well as to predict any potential geotechnical problem that might affect any current and/or future construction and urban development in the area.

## 2. The study area

Najran Region is situated in the southwestern part of Saudi Arabia; bordered to the east by the Empty Quarter Desert, the Asir region to the west, both Riyadh and the Eastern Provinces to the north, and the Republic of Yemen to the south. Najran region, which has an area of about 149,511 km<sup>2</sup>, is considered one of the fastest-growing southern regions in Saudi Arabia. Its population has increased nearly 2 times from 300,994 in 1992 to 595,705 in 2018 (Saudi General Authority for Statistics, 2018). The Geomorphology of Najran Province can be classified into three major geomorphological units: i) high-mountain areas in the west, ii) floodplain areas with alluvial deposits along Wadi Najran, and (iii) eastward dominating dunes along the Empty Quarter as shown in Fig. 1b.

The study area is located within the dunes unit to the east of Najran City occupying a major part of Khobash district. It lies between 17°31'16.00" and 17°31'47.926" North and

44°29'10.62" and 44°31'08.686" East (Fig. 1c). The study area has an area of about 1.5 km<sup>2</sup> with a length of about 2000 m and a width of approximately 750 m as shown in Fig. 1c.

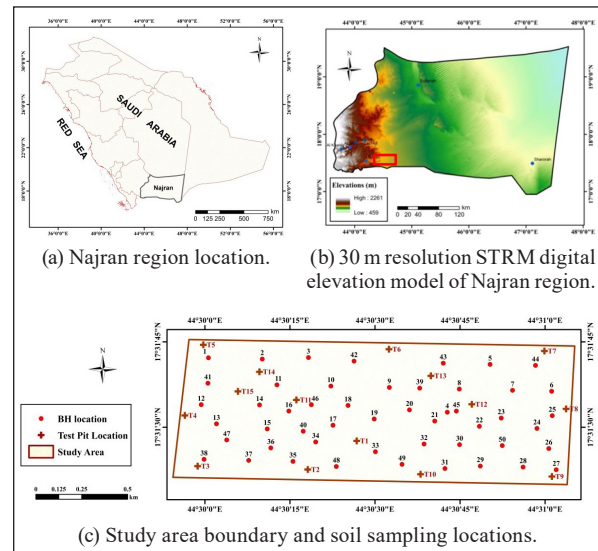


**Figure 1.** Study area location, geomorphology, geology (a and b), and soil sampling locations (c).

In terms of geology, the rocks in Najran Region belong to the Precambrian and consist of igneous rocks, as well as some stratified rocks of the Cambrian–Ordovician Wajeed sandstone, and occasional Tertiary bedrock (Shanti, 1993; Vincent, 2008; Stern and Johnson, 2010) as shown in Fig. 1b. Alluvial deposits along Wadi Najran as well as dunes are considered Quaternary deposits (Shanti, 1993).

## 3. Data and methodology

In this research, the geotechnical investigation involved the following three main stages: i) geotechnical field investigation; ii) geotechnical laboratory testing; and iii) Geotechnical data modeling and visualization

### 3.1 Geotechnical field investigation

#### 3.1.1 Reconnaissance field visit

Based on a reconnaissance field visit, it was found that the ground surface of the study area is almost flat covered by dry sand particles and its southern boundary is adjacent to a strategic Najran-Sharourah highway linking Saudi Arabia and Yemen (Figs. 1 and 2). Therefore, preliminary geotechnical investigation for such an area is crucial for urban planning and commercial development plans.

#### 3.1.2 Subsurface soil sampling

The study area has an area of about 1.5 km<sup>2</sup> estimated using ArcGIS technology. 50 random sampling locations were selected to cover this area to conduct a shallow borehole drilling process up to 10 m of depths investigating its geotechnical properties. These boreholes, denoted hereafter as BH (Fig. 1), were prepared according to the American Society for Testing and Materials ASTM D4428 standards (ASTM, 1995) and drilled using a rotary mobile borehole drilling machine (ACKER mobile rig) with a hole diameter of 50.8 mm as shown in Fig. 2.



**Figure 2.** General view of the study area condition showing the used drilling rig machine for the SPT test and soil sampling

At each BH, boring was advanced to the desired intervals of depths, which were 1, 3, 5, 8, and 10 m sequentially as illustrated in the created 3D model (Fig. 3). The point of selecting those intervals of depths is to reflect the geotechnical properties and, thus, the ground conditions of the investigated depths for further foundation and construction purposes at different levels of depth. Subsequently, disturbed soil samples were collected at each interval of depth at each borehole with a total of 250 BH soil samples.

To measure soil compaction parameters (maximum dry density and corresponding optimum moisture content of soil) and for foundation investigation purposes as well, open test pits with a width of about 1.2 m and a length of roughly 2 m were excavated to 3 m of depth using Backhoe Loader Machine at 15 different locations over the study area (Figs. 3 and 4, 5). 15 disturbed soil samples were collected from these test pits, denoted hereafter as TP soil samples.

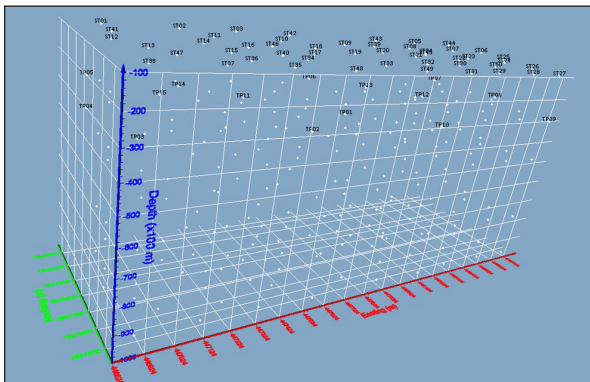


**Figure 3.** 3D- perspective view of the BH locations (ST locations) starting from the ground surface to 10 m depth with data points at 1, 3, 5, 8, and 10 m of depths using Voxler software. TPs represent the location of test pits. The vertical extension was exaggerated by one hundred times.

As a result, 265 soil samples were collected during the fieldwork (both 250 BH soil samples and 15 TP soil samples). All the collected samples were kept in plastic bags, and then transferred to the geotechnical lab of Al-Jazzar Consulting Engineers Company, Najran City, to measure their geotechnical index properties.

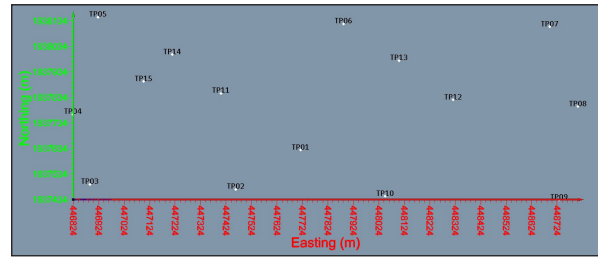


**Figure 4.** 2D map showing the spatial distribution of the 15 test pits (TP) across the study area



**Figure 5.** Excavation process of test pits in the study area

3.1.3 Standard penetration test (SPT)

Standard Penetration Test (SPT) is an important geotechnical method used to reflect the consistency and resistance of subsurface soils. During the BH drilling process, SPT was conducted according to ASTM D 1586. At each borehole (BH), the boring was, first, advanced to the desired depth level (1, 3, 5, 8, and 10 m) sequentially. Then, the split-spoon sampler attached to the drill rod was placed at the top of each testing point. The SPT-hammer, then, was dropped driving the sampler into the soil layer until reaching 15 cm of depth. This procedure was repeated two more times until 45 cm of total penetration was achieved. The total number of blows required to penetrate the last 30 cm depth is accounted as the “N-value”, which is used to determine the relative density of coarse soils ( $D_r$ ) and/or the strength of stiff cohesive soils based on the type of soil encountered (Table 1). All the results of the SPT (N-Value) are listed in Table 2.

**Table 1.** N-Value of SPT and its corresponding relative density of coarse soils (Modified after Rogers, 2006)

N-Value	D%	Description	Symbol
Less than 4	Less than 15	Very loose	VL
4 – 10	15 – 60	Loose	L
11 – 30	61 – 75	Medium	MD
31 – 50	76 – 90	Dense	D
Over 50	Over 90	Very Dense	VD

**Table 2.** Geotechnical Lab results of BH soil samples at depths 1, 3, 5, 8, and 10 m

St. No.	1 m of Depth				3 m of Depth				5 m of Depth				8 m of Depth				10 m of Depth			
	Soil Type	SPT Results		w%	Soil Type	SPT Results		w%	Soil Type	SPT Results		w%	Soil Type	SPT Results		w%	Soil type	SPT Results		w%
		N	D <sub>r</sub>			N	D <sub>r</sub>			N	D <sub>r</sub>			N	D <sub>r</sub>			N	D <sub>r</sub>	
1	SP	15	MD	5.6	SP	43	D	7.1	SP	54	VD	2.9	SP	55	VD	12.3	SP-SM	70	VD	9.1
2	SP	26	MD	12.3	SP-SM	26	MD	11.1	SP-SM	30	MD	13.5	SP	52	VD	15.6	SP-SM	54	VD	15.5
3	SP-SM	22	MD	11.9	SP-SM	36	D	13.6	SP-SM	59	VD	16.3	SP-SM	57	VD	14.2	SP	59	VD	18.5
4	SP	16	MD	14.3	SP	45	MD	9.3	SP-SM	57	VD	12.6	SP-SM	76	VD	10.5	SP-SM	75	VD	14.1
5	SP-SM	23	MD	15.2	SP-SM	43	D	18.2	SP-SM	50	D	18.2	SM	50	D	12.5	SM	68	VD	12.7
6	SP-SM	32	D	18.3	SP-SM	45	D	15.9	SM	58	VD	17.3	SP	53	VD	12.1	SP-SM	62	VD	16.4
7	SM	30	MD	12.1	SM	24	MD	12.9	SP	27	MD	11.5	SM	53	VD	11.9	SP	62	VD	11.8
8	SP	18	MD	11.8	SP	27	MD	8.9	SP-SM	55	VD	11.2	SM	60	VD	9.6	SP	54	VD	11.5
9	SP-SM	22	MD	14.9	SP-SM	29	MD	8.8	SP-SM	43	D	15.6	SP	51	VD	18.3	SP-SM	65	VD	17.4
10	SP	44	D	10.9	SP-SM	34	D	13.5	SP-SM	50	D	13.5	SP	63	VD	10.9	SP-SM	63	VD	9.8
11	SP-SM	17	MD	12.5	SP-SM	26	MD	14.2	SP	47	D	12.7	SP-SM	70	VD	12.7	SM	80	VD	16.9
12	SP	23	MD	8.7	SP-SM	19	MD	9.8	SM	55	VD	11.5	SM	52	VD	10.1	SP-SM	56	VD	6.7
13	SP	30	MD	11.5	SP	35	D	13.8	SP	60	VD	14.6	SM	74	VD	15.6	SP	72	VD	17.9
14	SP	24	MD	6.4	SP	22	MD	9.1	SP	25	MD	14.4	SM	37	D	6.8	SP	44	D	7.9
15	SP	27	MD	16.4	SP	24	MD	15.5	SP-SM	42	D	14.2	SM	61	VD	16	SP-SM	78	VD	20.1
16	SM	31	D	12.9	SM	28	D	15.5	SM	49	D	11.6	SM	50	D	5.9	SP-SM	76	VD	4.71
17	SP-SM	20	MD	13.8	SP-SM	13	MD	11.2	SM	33	D	11.3	SM	44	D	11.9	SM	48	D	13.4
18	SP	22	MD	11.5	SP	26	MD	14.4	SP-SM	50	D	13.1	SP	80	VD	7.7	SM	82	VD	14.1
19	SP	24	MD	9.5	SP	24	MD	8.6	SP-SM	25	MD	6.9	SP-SM	45	D	5.4	SP-SM	48	D	9.2
20	SP	23	MD	11.3	SP	25	MD	9.1	SM	47	D	8.7	SP-SM	42	D	11.1	SP-SM	40	D	12
21	SP	20	MD	12.9	SP	29	MD	14.3	SP	41	D	14.4	SP-SM	50	D	14.4	SP-SM	60	VD	12.9
22	SP	26	MD	5	SP	28	MD	11.4	SP-SM	35	D	8.9	SP	41	D	9.4	SM	40	D	11.2
23	SP-SM	31	D	13	SP-SM	32	D	11.1	SP-SM	41	D	11.9	SM	45	D	15.5	SP-SM	56	VD	17.2
24	SP-SM	20	MD	7.8	SP-SM	28	MD	15.4	SP-SM	48	D	6.6	SM	51	VD	12.9	SP-SM	44	D	12.9
25	SM	26	MD	15.9	SM	27	MD	17.6	SP-SM	50	D	10.5	SM	67	VD	16.9	SP-SM	75	VD	12.11



3.1.4 Groundwater investigation

During the drilling of the shallow boreholes process as well as the excavation of the test pits, groundwater was not encountered in the study area.

3.2 Geotechnical lab testing

All the geotechnical tests of the collected subsurface soil samples were performed according to the American Society for Testing and Materials (ASTM, 1995). As aforementioned, two types of disturbed subsurface soil samples were collected in this research: 250 BH soil samples and 15 TP soil samples (in a total of 265 soil samples).

3.2.1 Laboratory testing of BH soil samples

250 subsurface soil samples were collected from all 50 BH locations at five different successive depth levels (1, 3, 5, 8, and 10 m). All those collected samples were subjected to the following lab tests:

- Natural water content test according to ASTM D 2216.
- Soil grain size analysis according to the ASTM D422.
- Soil classification using the Unified Soil Classification System (USCS) and according to ASTM D2487. For those coarse soils containing significant portions of fine particles, fine soil particles were identified according to both ASTM D4318 (Atterberg Limits test). The Atterberg limits test is commonly used as an integral part of several engineering classification systems such as USCS to characterize fine-grained fractions of soils.
- Modified Proctor Compaction test according to ASTM D 1557.

Although the SPT was conducted for all the soils at the intervals of desired depths, a direct shear box test was also conducted according to ASTM D3080 for those soil samples collected at a depth of 3 m but at only twelve selected borehole locations as shown in Fig. 6. The purpose of conducting this test was to measure the strength of the soil of the investigated area and thus to create more accurate and reliable measurements about the subsurface conditions of the area. All the geotechnical lab results of the BH soil samples are listed in Tables 2 and 3.

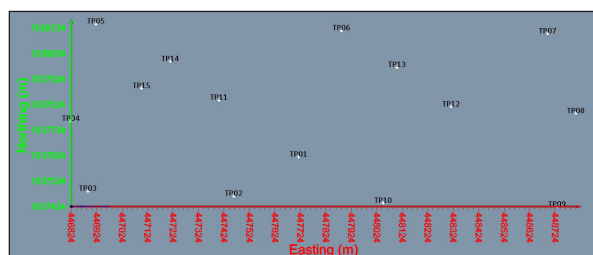


Figure 6. 2D map showing the location of the 12 BH stations selected to measure the shear strength of soils

3.2.2 TP soil samples

All the 15 collected TP soil samples were subjected to the following lab tests:

- Soil grain size analysis according to the ASTM D422
- Soil classification using the Unified Soil Classification System (USCS) and according to ASTM D2487 and ASTM D4318.
- Modified Proctor Compaction test according to ASTM D 1557.

Soil types and maximum dry density ( $\rho_{dry}$ ) and the corresponding optimum moisture content (OMC) were determined for all the 15 TP soil samples as listed in Table 3.

Table 3. Soil types and their compaction parameter values at the excavated test pits at 3 m depth in the study area

St. No.	Soil Type	$\rho_{dry}$ (g/cm <sup>3</sup> )	OMC %
TP1	SP	2.15	7.20
TP2	SP	2.15	7.00
TP3	SP-SM	2.12	7.30
TP4	SP	2.14	7.50
TP5	SP	2.09	8.60
TP6	SP	2.01	8.70
TP7	SP	2.19	8.20
TP8	SP	2.14	7.70
TP9	SP	2.16	7.60
TP10	SP	2.17	7.50
TP11	SP	2.15	7.70
TP12	SP-SM	2.01	9.70
TP13	SP	2.12	7.40
TP14	SP	2.10	7.10
TP15	SP	2.18	8.20
Min.		2.01	7.00
Max.		2.19	9.70
Ave		2.13	7.83

3.3 Geotechnical data modeling and visualization

Three-dimensional models of the obtained results of natural water content, soil types, SPT results (N-Value), relative density ( $D_r$ ), maximum dry density ( $\rho_{dry}$ ), optimum moisture content (OMC), and shear strength were created using the Voxler v.3 software package (<http://www.goldensoftware.com/products/Voxler>).

In general, the first step in the 3D modeling process is data preparation. In this research, each set of geotechnical data was arranged in a format compatible with input to the software – including the 3D coordinates and corresponding geotechnical properties of each data point. Next, the Gridding function was used to convert the input data into a lattice node interpolated file based on the defined gridding parameters. Finally, the VolRender function was used to generate the 3D models by choosing the appropriate color scales that best highlight the spatial variation in geotechnical properties across the study area. Similarly, the Oblique-Image tool was used to generate 2D models of the study area, where applicable - which were 2D slices of the created 3D models at the desired various levels of depths (1, 3, 5, 8, and 10 m consecutively) as will be illustrated later in the next sections.

4. Results and discussion

4.1 Soil Grain Size Analysis and Soil Types

Based on the grain size analysis results of the 265 collected subsurface soils, only three main types of soil grain size were identified in the investigated area: sand (61 – 99%), silt (0 – 26%), and gravel (0 – 23%) with an average of 87.24%, 7.81%, and 4.70%, respectively. The absence of clay particles was a strong indicator of the low plasticity, or even non-plasticity, character that those soils may have. These results reflected a significant range of variation in soil

particle sizes which certainly affects the soil engineering behavior vertically and horizontally across the study area.

In terms of soil classification, it is found that only sandy soil covers the whole investigated area. Precisely, three different soil types have been identified: poorly graded sand (SP), poorly graded sand with silt (SP-SM), and silty sand (SM) as listed in Tables 2 and 3. As noticed, this soil is poorly graded (well sorted) which is generally characterized by higher porosity compared to well-graded sand soil.

The other observation is that SP soil occupies the major portion of the first three-meter depths of investigation with a percent of occurrence ranging between 46% and 86.67% and, then, this occurrence decreases gradually with increasing depth of investigation (Table 4). This spatial variation was portrayed through the created geotechnical models (Fig. 7). These created 2D and 3D geotechnical models showed that SP soil particles are concentrated mainly in the western and the middle parts of the study area.

**Table 4.** Frequency and percent of identified soil types of the investigated depths of the study area.

	No. of Samples	Soil Type	Investigated Depth level									
			1 m		3 m		5 m		8 m		10 m	
			Freq.	%	Freq.	%	Freq.	%	Freq.	%	Freq.	%
BH samples	250	SP	28	56	23	46	15	30	11	22	6	12
		SP-SM	16	32	21	42	25	50	20	40	33	66
		SM	6	12	6	12	10	20	19	38	11	22
TP samples	15	SP			13	86.67						
		SP-SM	-	-	2	13.33						
		SM			0	0						
BH + TP samples at 3 m of depth	65	SP			36	55.38						
		SP-SM	-	-	23	35.38						
		SM			6	9.24						

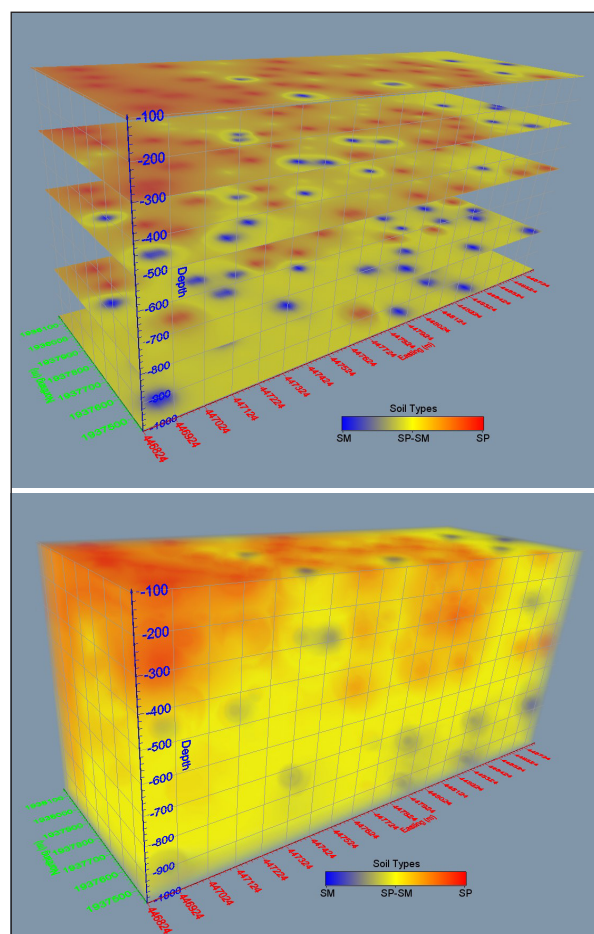


**Figure 7.** 2D slices (above) and 3D model (below) of the spatial distribution of soil types in the investigated area.

Moreover, it can be noted that SP-SM and SM soil types occur a little more at the depth of 3 m compared to the first investigated meter of depths (Table 4; Fig.7). This occurrence of silty sand was more significantly observed at the depths below 3 m where SP-SM soil occupies the major parts covering 40% and up to 66% of those investigated depth (Table 4, Fig.7).

Furthermore, as shown in Fig. 7, the 2D geotechnical models of soil types depicted the horizontal spatial distributions of the SM soil where a significant occurrence of it (38%) can be shown at the depth of 8 m (Table 4).

According to the created geotechnical models (Fig. 7) as well as the results listed in Table 4, it can, briefly, be concluded that the SP soil is the dominant soil type that occurs within the first three meters of depth. Then, SP-SM soil type is the one that significantly occurred within the rest of the investigated depth (below 3 m) but with the presence of a considerable amount of SM soil (38%) particularly at the depth of 8 m of investigation (Fig.7, Table 4).

4.3 Natural water content

Because natural water content (w) has a profound effect on soil engineering behavior, all the 250 BH soil samples were examined to determine their natural water content.

The current geotechnical investigation showed that the water content values of the soils in the study area were between 2.9 and 20.1% with an average of 12.26% and a range of 17.2%. In general, such a wide range in water content values of the soils should be taken into consideration for any urban planning and construction that may take place in the area.

Based on the results listed in Table 2, the range of water content (w) values was almost constant for those samples collected at depths 1m (w = 5% – 18.3%), 3m (w = 4.9% – 18.2%), and 8 m (w = 5.4% – 18.3%) with a range value of about 13%. The highest range of water content recorded in the area was at a depth of 5 m (w = 2.9% to 18.2% with a range of 15.3%) and a depth of 10 m (w = 4.71% to 20.10% with a range of 15.39%). The significant vertical variation of water content values especially at depths below 3 m can be referred to the presence of a considerable portion of silt particles where SP-SM and then SM soil types are the dominant types below 3 m of depth (Tables 2 and 4; Figs. 8 and 7). Based on the created geotechnical models (Fig. 8), the most common range of water content measured within the investigated depths was between 9% and 16% with a range of 7.

4.4 Standard penetration test (N-value and relative density of soil)

SPT results (N-value) are mainly used to estimate consistency, strength, and, in some cases, soil compressibility. In general, the SPT results (N-value) of the investigated area ranged between 13 and 85 representing a range of soil relative density ( $D_r$ ) of medium to very dense soils as listed in Tables 1 and 2.

N-value was correlated to relative density and then summarized as listed in Table 5. According to the measured relative density, three types of soils have been identified in the study area: medium-dense soil (MD-soil), dense soil

(D-soil), and very dense soil (VD-soil). It is found that, within the first three meters of depths, all the soils showed a relative density level of medium (MD) to dense (D). In other words, SPT results revealed that there was no very dense soil (VD) encountered within the first three meters of depths of investigation. In contrast, very dense soil was encountered below 3 m of depths, particularly at depths of 8 m and 10 m where no medium-dense soil was encountered at all (Table 5; Fig. 9).

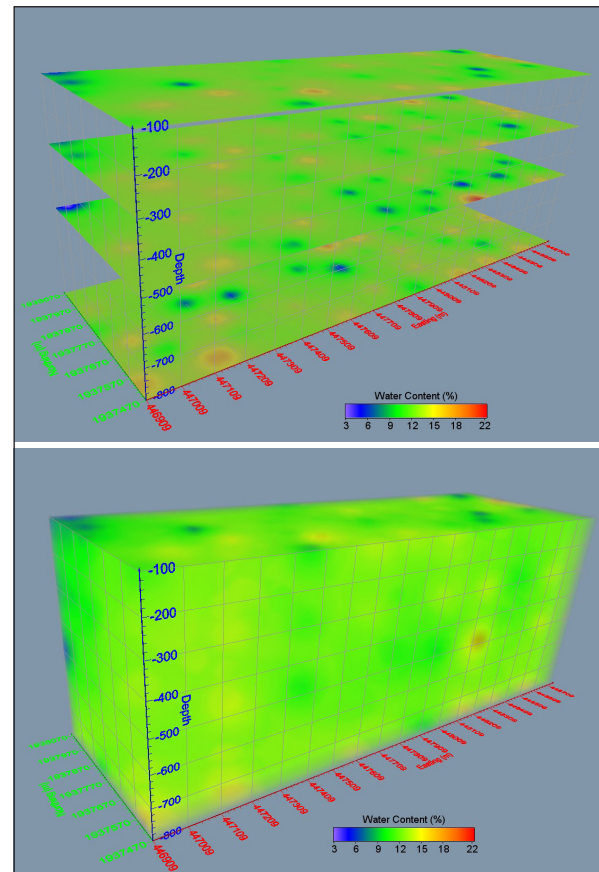


Figure 8. 3D Model (above) and 2D slices (below) of the spatial distribution of water content in the investigated area

Table 5. Estimated frequency and percent of each relative density type ( $D_r$ ) of the 250 BH soil samples.

$D_r$ Type	Investigated Depth										
	1 m deep		3 m deep		5 m deep		8 m deep		10 m deep		
	Freq.	%	Freq.	%	Freq.	%	Freq.	%	Freq.	%	
MD	44	88	36	72	8	16	-	-	-	-	
D	6	12	14	28	31	62	22	44	14	28	
VD	-	-	-	-	11	22	28	56	36	72	
$D_r$ Zone	MD- Soil Level			D- Soil Level				VD- Soil Level			

As the depth of investigation increases, the density of soils increases which can be due to the overburden of the above layers of soils as well as because of increasing fine soil (silt) particles in those soils occurring below 3 m of depth (Figs. 7 and 9).

In general, (N-value), the vertical extension of the study area can be divided into three main zones based on the measured relative densities as follows (Table 5, Fig. 9):

i- MD-Soil Zone: This zone of density was observed within the first three meters of the investigated depths where N- N-values were between 13 and 46 while the corresponding relative density was medium dense to dense soil (MD – D). Within the depth of 1 m, it can be observed that 44 (88%) out of 50 soil samples have medium-dense relative density (MD). Additionally, 36 soil samples (72%) were characterized as MD as well at the depth of 3 m (Table 5, Fig 9). Therefore, the majority of soils that occur within the first three meters

of investigated depths are medium dense where the SP soil is the dominant soil type (Table 4; Figs. 7 and 9).

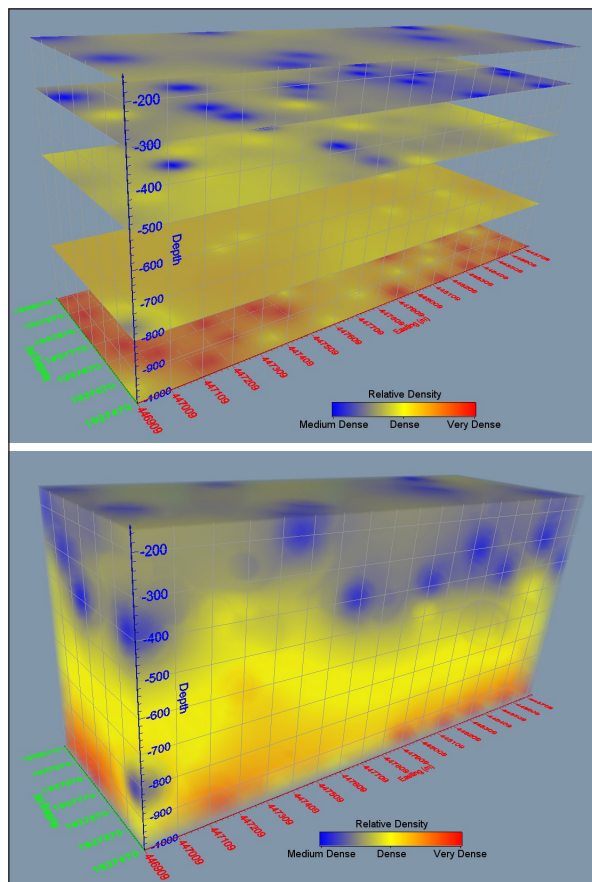


**Figure 9.** 2D Model (above) and 3D slices (below) of the spatial distribution of relative density ( $D_r$ ) in the investigated area.

ii- D-Soil Zone: This zone of density was observed at only 5 m of depth where the soils had a range of N-value of 25 to 72 with a relative density ranging from medium (MD) to very dense (VD). Although, 8 soil samples were identified as medium dense (MD) and 11 samples measured as very dense (VD), the majority of soil samples (31 samples) with a percent of 62% were measured as dense soil (D) at only this level of depth (Fig. 8, Table 5). The other remarkable observation is that this zone is the only zone that has the

widest range of relative density (medium dense to very dense soil) where all the three identified soil types (SP, SP-SM, and SM) have significantly occurred within this level of depths (Table 4; Figs. 7, 9)

iii- VD-Soil Zone: This zone of density was encountered in the last two levels of depths of investigation (8m and 10m depths) where the observed N-values of soils fell between 31 and 85 with a relative density of dense (D) to very dense (VD). However, very dense soils represent 56% and 72% of the soils at 8 m and 10 m of depth, respectively. Accordingly, this zone is characterized by its high relative density (very dense soil) (Table 5, Fig.9). It should be noted that there is no medium-dense soil was detected at this level of depth (Table 5).

As aforementioned SP-SM soil and then SM soil were the most encountered soil types below the depth of 3m, and thus the increasing density within the other investigated levels of depths (5, 8, and 10 m) can be related to the increasing of fine particles (silt grain fraction) at those depths (Table 4; Fig. 7).

#### 4.5 Shear strength of soil

As aforementioned 12 subsurface soil samples were collected from different 12 BH locations at only a depth of 3m to measure soil shear strength utilizing direct shear test (Fig. 6).

The results indicated that the shear strength of the soils mainly resulted from their internal friction angle ( $\phi$ ) since their cohesion values are all less than 1 kg/cm<sup>2</sup>. All the examined soil samples have very low cohesion strength values not exceeding 0.24 kg/cm<sup>2</sup> (Table 6, Fig. 10). Friction angle ( $\phi$ ) values of these soils ranged between 23° and 32° with an average of 26.5°.

According to the created horizontal spatial variation map (2D model) of the measured internal friction angles as depicted in Fig. 11, it can be noticed that most parts of the soil had a friction angle that varies between 25° and 28° where SP soil is the dominant type of soils occupying the major part of the investigated study area but at the depth of 3 m as illustrated in Fig. 7 as well.

**Table 6.** Soil shear strength measurements conducted for soils at 3 m of depth.

BH No. (St. No.)	Soil type	Friction angle ( $\phi$ in degrees)	Cohesion (kg/cm <sup>2</sup> )	BH No. (St. No.)	Soil type	Friction angle ( $\phi$ in degrees)	Cohesion (c, kg/cm <sup>2</sup> )
1	SP	29	0.06	28	SP-SM	24	0.14
6	SP-SM	23	0.15	36	SP	28	0.17
8	SP	26	0.09	41	SP	28	0.20
9	SP-SM	26	0.23	44	SP-SM	26	0.21
10	SP-SM	25	0.18	47	SP	24	0.24
22	SP	27	0.14	50	SM	32	0.05

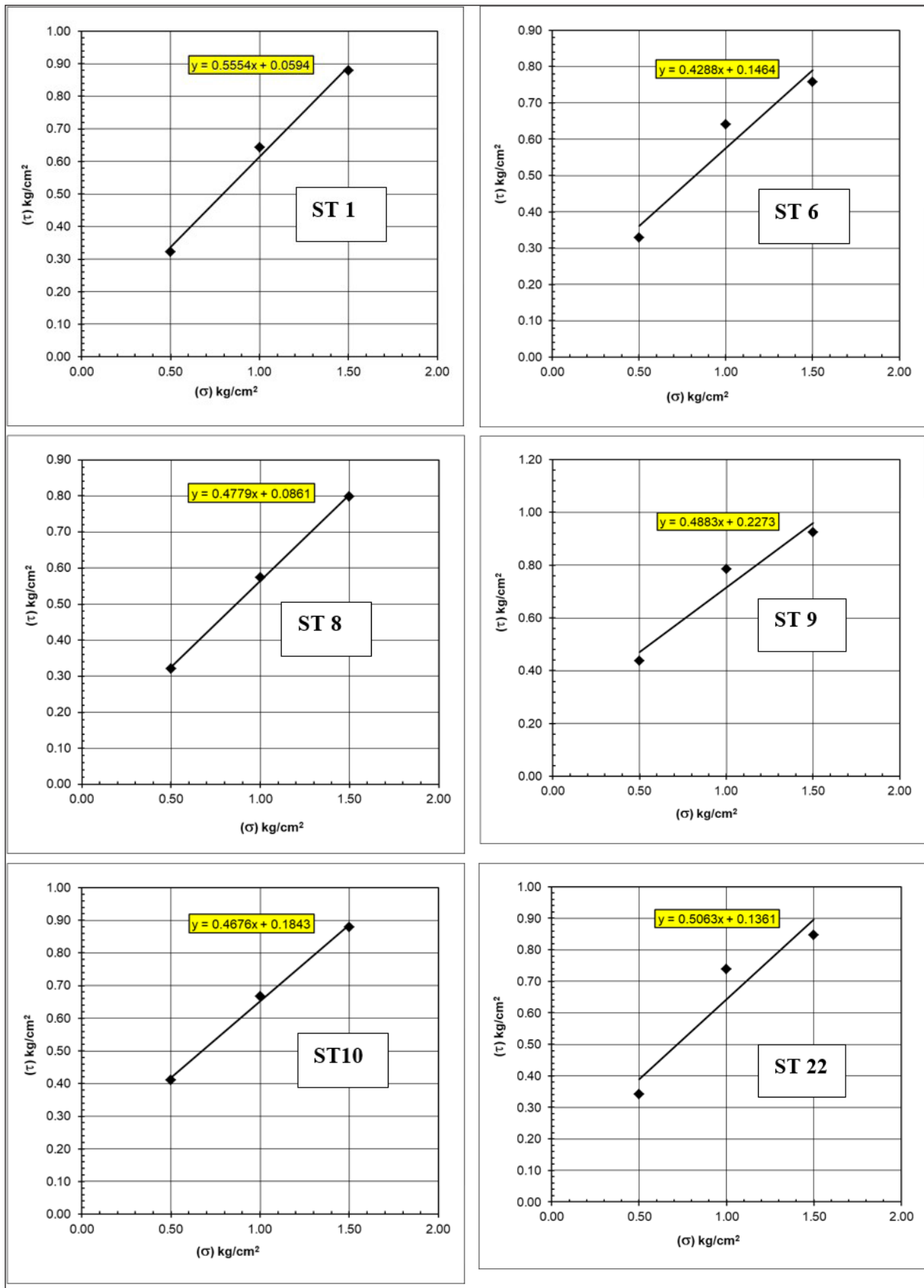


Figure 10. Shear strength curves of the 12 BH soil samples collected at 3 m depth.

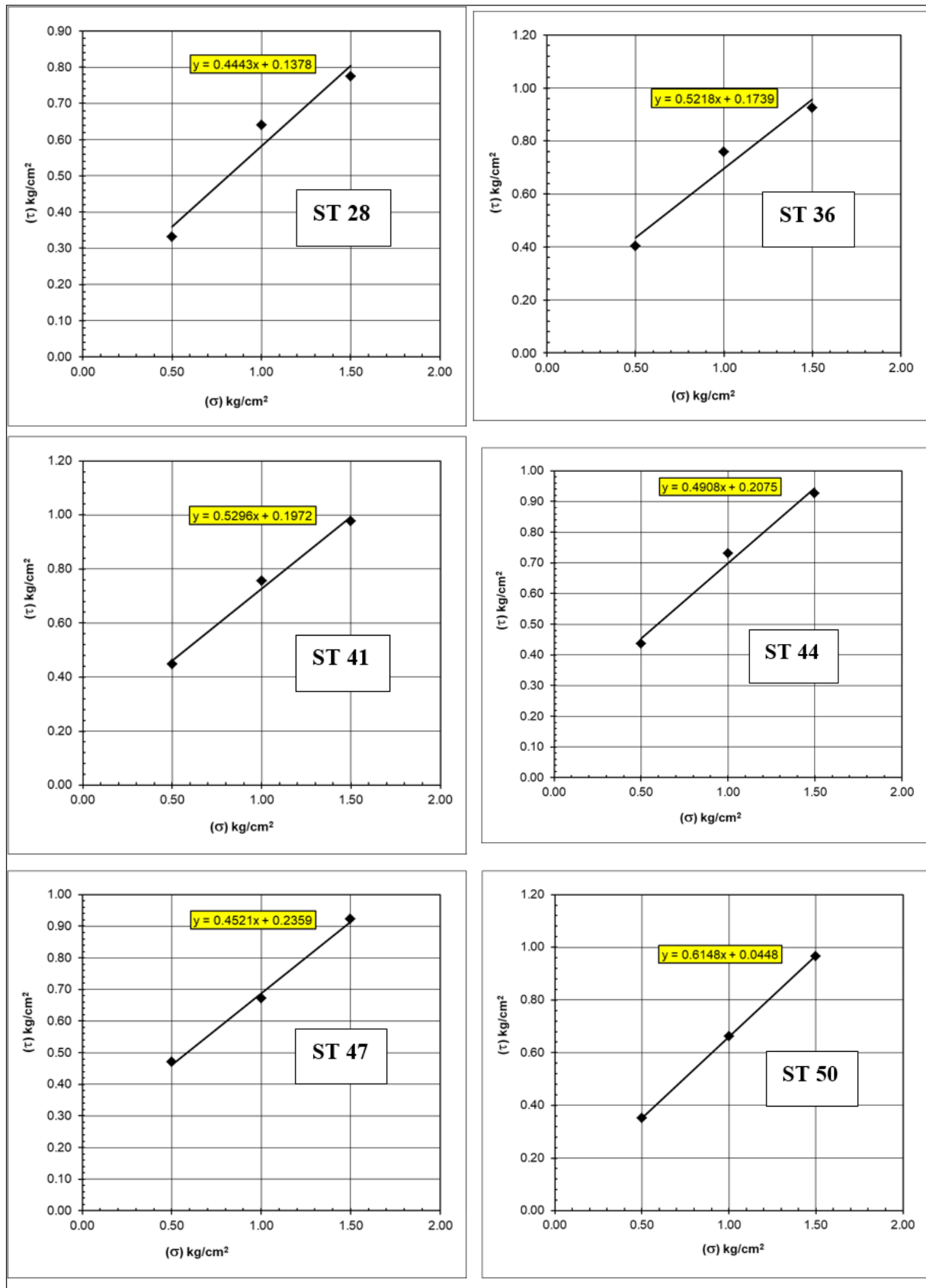
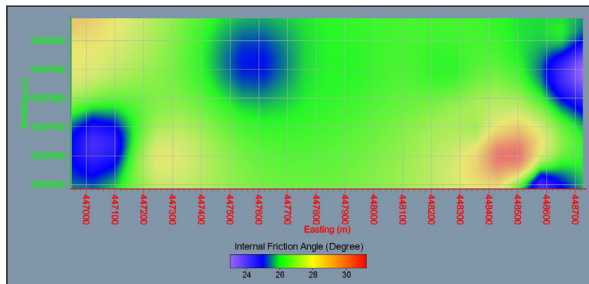


Figure 10. (continued) Shear strength curves of the 12 BH soil samples collected at 3 m depth.



**Figure 11.** 2D slice of horizontal distribution of strength of soil (internal friction angle) at the 3 m depth of the investigated area.

#### 4.6 Soil compaction parameters (Maximum dry density and OMC)

The results of the modified proctor compaction test, which was conducted on the collected 15 TP soil samples, showed that the maximum dry density ( $\rho_{dry}$ ) ranged between 2.01 and 2.19 g/cm<sup>3</sup> with an average of 2.12 g/cm<sup>3</sup> while their corresponding range of optimum moisture content (OMC) was 7.0 - 9.7% with an average of 7.83% (Table 3).

As shown in Fig. 12, the produced 2D geotechnical models of soil compaction parameters, it can be concluded that the best range of OMC to obtain the possible highest range of maximum dry density (2.10 to 2.20 g/cm<sup>3</sup>) is 7.0 to 8.0 % of moisture content. Furthermore, when checking the horizontal distribution of soil types at this depth as shown in Fig.7, it can be concluded that SP soil and then SP-SM soil are those soils on which maximum dry density can be achieved (Figs 7 and 12).

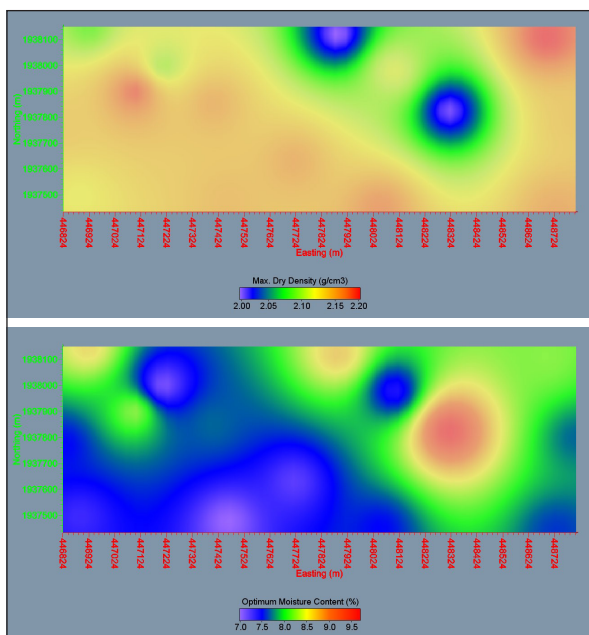


**Figure 12.** 2D spatial distributions of maximum dry density (above) and corresponding OMC percents (below) at the depth of 3 m of the investigated area.

## 5. Conclusions

According to the grain size analysis results of the 265 collected subsurface soils at different depths (1, 3, 5, 8, and 10 m), only sand, silt, and gravel particles have been identified with the absence of clay particles. As a result, the soils were classified into: SP, SP-SM, and SM soils.

Based on the created geotechnical models, SP soil was the dominant soil type that occurs within the first three meters

of depth where most soils are medium dense (MD zone). It was also found that within this depth of investigation, most soils have friction angles that vary between 25° and 28°; and SP soil and SP-SM soils are those types of soils on which maximum dry density can be achieved but within a range of OMC of 7.0 – 9.7%.

At depths below 3 m, SP-SM soil type has significantly occurred but with a considerable amount of SM soil particularly at 8 m of depth. Furthermore, it was observed most soil samples at 5 m of depth have dense density (D zone) while the majority of soil samples below 5 m of depth reflected very dense density (VD zone). Moreover, the produced geotechnical models depicted significant vertical variation of water content at depths below 3 m where SP-SM and, then, SM soil types are the dominant types.

In sum, the created 2D and 3D geotechnical models were effective and valuable in the visualization of spatial variations in the geological properties of the subsurface soil of the study area. Using such models has made correlating and interpreting geotechnical properties with each other, and even within each property itself, an easy and effective task to track spatial variations in any direction; therefore, the geotechnical behavior of subsurface soil can be predicated in a time manner geoen지니어ing purposes.

## Acknowledgment

The authors would like to acknowledge Al-Jazzar Consulting Engineers Company for their technical support and providing some raw geotechnical data. In addition, the authors would also like to thank those unknown reviewers of the JJEES for their valuable remarks.

## References

- Abd El Aal AK, Kamel M, Al-Homidy A (2019) Using Remote Sensing and GIS Techniques in Monitoring and Mitigation of Geohazards in Najran Region, Saudi Arabia. *Geotech Geol Eng* 37: 3673–3700. <https://doi.org/10.1007/s10706-019-00861-w>.
- Abd El Aal AK, Rouaiguia A (2020) Determination of the Geotechnical Parameters of Soils Behavior for Safe Future Urban Development, Najran Area, Saudi Arabia: Implications for Settlements Mitigation. *Geotech Geol Eng* 38:695-712. <https://doi.org/10.1007/s10706-019-01058-x>.
- Abd El Aal AK, Nabawy BS, Aqeel A, Abidi A (2020) Geohazards assessment of the karstified limestone cliffs for safe urban constructions, Sohag, West Nile Valley, Egypt. *Journal of African Earth Sciences* 161. <https://doi.org/10.1016/j.jafrearsci.2019.103671>.
- Aqeel A, Zaman H, Abd El Aal A (2019) Slope Stability Analysis of a Rock Cut in a Residential Area, Madinah, Saudi Arabia: A Case Study. *Geotech Geol Eng* 37:1765–1778. <https://doi.org/10.1007/s10706-018-0720-7>.
- Ayodele O S, Ajigo I O (2020) Geological Mapping and Gemstones prospecting in Deformed Precambrian Rocks, East of Okemesi Fold Belt, Southwestern Nigeria. *The Jordan Journal of Earth and Environmental Sciences (JJEES)* 11 (4): 290-301
- Aghamolaie I, Lashkaripour GR, Ghafoori M, Moghaddas NH (2019) 3D geotechnical modeling of subsurface soils in Kerman city, southeast Iran. *Bull. Eng Geol Environ* 78: 1385. <https://doi.org/10.1007/s10064-018-1240-7>.
- Bell FG (2007) *Engineering Geology*, 2nd ed. Elsevier, Oxford.

- Breyse D, Niandou H, Elachachi SM, Houy L (2005) A generic approach to soil structure interaction considering the effects of soil heterogeneity. *Géotechnique* 55(2):143–150. <https://doi.org/10.1680/geot.2005.55.2.143>.
- Dong M, Neukum C, Hu H, Azzam R (2015) Real 3D geotechnical modeling in engineering geology: a case study from the inner city of Aachen, Germany. *Bull Eng Geol Environ* 74(2):281-300. <https://doi.org/10.1007/s10064-014-0640-6>.
- Donghee K, Kyu-Sun K, Seongkwon K, et al (2012) Assessment of geotechnical variability of Songdo silty clay. *Eng Geol* 133–134:1–8. <https://doi.org/10.1016/j.enggeo.2012.02.009>.
- Ford J, Burke H, Royse K, Mathers S (2008) The 3D geology of London and the Thames Gateway: a modern approach to geological surveying and its relevance in the urban environment, In the 2nd European Conference of International Association for Engineering Geology, Madrid, Spain, 15–20 Sept 2008.
- Hack R, Orlic B, Ozmutlu S, Zhu S, Rengers N (2006) Three and more dimensional modelling in geoengineering. *Bull Eng Geol Environ* 65:143-153. <https://doi.org/10.1007/s10064-005-0021-2>.
- Kanu M O, Meludu O C, Oniku S A (2013) A Preliminary Assessment of Soil Pollution in Some Parts of Jalingo Metropolis, Nigeria Using Magnetic Susceptibility Method. *The Jordan Journal of Earth and Environmental Sciences (JJEES)* 5 (2): 53-61
- Khallouf A, AlHinawi S, AlMesber W et al (2020) Digital Mapping of Soil Properties in the Western-Facing Slope of Jabal Al-Arab at Suwaydaa Governorate, Syria. *The Jordan Journal of Earth and Environmental Sciences (JJEES)* 11 (3): 193-201
- Kolat Ç, Doyuran V, Ayday C, LütfiSüzen M (2006) Preparation of a geotechnical microzonation model using geographical information systems based on multicriteria decision analysis. *Eng Geol* 87(3–4):241–255. <https://doi.org/10.1016/j.enggeo.2006.07.005>.
- Kolat Ç, Ulusay R, LütfiSüzen M (2012) Development of geotechnical micro zonation model for Yenisehir (Bursa, Turkey) located at a seismically active region. *Eng Geol* 127:36–53. <https://doi.org/10.1016/j.enggeo.2011.12.014>.
- Massoud A (2016) Geotechnical site suitability mapping for urban land management in Tanta District, Egypt. *Arab J Geosci* 9:340. <https://doi.org/10.1007/s12517-016-2363-4>.
- Mendes RM, Lorandi R (2008) Analysis of spatial variability of SPT penetration resistance in collapsible soils considering water table depth. *Eng Geol* 101:218–225. <https://doi.org/10.1016/j.enggeo.2008.06.001>.
- Parsons RL, Frost JD (2002) Evaluating Site Investigation Quality using GIS and Geostatistics. *Journal of Geotechnical and Geoenvironmental Engineering* 128(6):451-461. [https://doi.org/10.1061/\(ASCE\)1090-0241\(2002\)128:6\(451\)](https://doi.org/10.1061/(ASCE)1090-0241(2002)128:6(451)).
- Rogers JD (2006) Subsurface Exploration Using the Standard Penetration Test and the Cone Penetrometer Test. *Environmental and Engineering Geosciences* 12 (2):161-179. <https://doi.org/10.2113/12.2.161>.
- Royse KR, Rutter H, Entwisle D (2009) Property attribution of 3D geological models in the Thames Gateway, London: new ways of visualizing geoscientific information. *Bull Eng Geol Environ* 68:1–16. <https://doi.org/10.1007/s10064-008-0171-0>.
- Saudi General Authority for Statistics (2018) “Saudi Arabia Regions and Major Cities: Population Statistics, Maps, Charts, and Weather.” <http://www.citypopulation.de/en/saudiarabia/cities/> (Oct. 12, 2022).
- Shanti AM (1993) *Geology of the Arabian Shield*. King Abdulaziz University Press, Jeddah, Saudi Arabia
- Stern R, Johnson P (2010) Continental lithosphere of the Arabian plate: a geologic, petrologic and geophysical synthesis. *Earth Sci Rev* 101:29–67. <https://doi.org/10.1016/j.earscirev.2010.01.002>.
- Tang C, Xu Q (2009) Approach on geohazards risk management for urban in a strong seismic zone. *Journal of Engineering Geology* 17(1):56–61.
- Thierry P, Prunier-Leparmentier A, Lembezat C, et al (2009) 3D geological modeling at urban scale and mapping of ground movement susceptibility from gypsum dissolution: the Paris example (France). *Eng Geol* 105:51–64. <https://doi.org/10.1016/j.enggeo.2008.12.010>.
- Tobore A, Senjobi B, Oyerinde G, Bamidele (2023) Geospatial Soil Suitability Assessment for Maize (*Zea mays*) Production in Derived Savanna of Agricultural Research and Training, OYO STATE, Nigeria. *The Jordan Journal of Earth and Environmental Sciences (JJEES)* 14 (1): 9-18
- Vincent P (2008) *Saudi Arabia: an environmental overview*. Taylor and Francis, Netherlands.